Scientific paper

Comparative Molecular Field Analysis (CoMFA), Molecular Docking and ADMET Study on Thiazolidine-4-carboxylic acid Derivatives as New Neuraminidase Inhibitors

Lotfi Bourougaa, 1 Mebarka Ouassaf^{1,*} and Shafi Ullah Khan²

 1 Group of Computational and Medicinal Chemistry, LMCE Laboratory, University of Biskra, BP 145 Biskra 707000, Algeria

² Product and Process Innovation Department, Qarshi Brands Pvt. Ltd., Hattar Industrial Estate-22610, Haripur, KPK Pakistan

* Corresponding author: E-mail: nouassaf@univ-biskra.dz

Received: 03-04-2023

Abstract

The objective of this research was to create a 3D-QSAR CoMFA model for a set of twenty-five neuraminidase inhibitors containing thiazolidine-4-carboxylic acid derivatives and to identify a new potent neuraminidase inhibitor for the treatment of influenza. The statistical parameters of the generated model are excellent: $Q^2 = 0.708$, $R^2 = 0.997$. The external validation results were ($r_0^2 = 0.922$, K= 1.016, $R_{pred}^2 = 0.674$, $r_m^2 = 0.778$) indicating that the constructed model has good predictive power. Based on the contour map of the CoMFA model, we were able to propose six novel compounds with higher neuraminidase inhibitory activity than the most active compound. The six proposed molecules were submitted to molecular docking to analyse the bindings formed between the newly designed molecules and the neuraminidase. All of the proposed molecules were found to be more stable on the active site of neuraminidase than the reference molecule (1SJ). SwissADME was used to estimate the pharmacokinetic properties of each proposed molecule, while ProToxII and VEGA QSAR were used to investigate any potential toxicity. Finally, a reaction mechanism for synthesizing the six proposed compounds was described, which could potentially be explored further in the search for novel neuraminidase inhibitors. In conclusion, this study has identified potential candidates for the development of more effective neuraminidase inhibitors for the treatment of influenza.

Keywords: thiazolidine-4-carboxylic acid, Neuraminidase, influenza, 3D-QSAR, CoMFA, Molecular Docking, ADMET study.

1. Introduction

Influenza is a respiratory disease caused by the Orthomyxoviridae virus family. Every year, influenza viruses generate seasonal epidemics that mostly affect the adult population. 10-30% of sick people are hospitalized, and 3–15% die. Influenza symptoms include a sudden onset of high temperature, aching muscles, headache, severe exhaustion, a nonproductive cough, a sore throat, and a runny nose.² The variation of influenza viruses can develop in a pandemic, posing a major danger to public health.3 Neuraminidase (NA) is a glycoprotein located in the envelope of the influenza virus that plays a critical role in the process of infecting and spreading amongst human host cells.4 Neuraminidase is an important target of drug design for the treatment of influenza infections because to its involvement in viral propagation and it's largely preserved

active site.⁵ Neuraminidase inhibitors (NAI) represent the only extensively approved class of antiviral medications used for the treatment and prevention of seasonal influenza.6 Oseltamivir is widely utilized, whereas Zanamivir, Peramivir, and Laninamivir are used in fewer nations concurrently.7 NAIs are the most often given anti-influenza medications nowadays, they have been shown to be beneficial in speeding viral clearance, lowering clinical disease duration, and decreasing hospital stay and death.8

Computer-Aided Drug Design (CADD) is the process of using computer methods and resources to design and identify novel potential pharmaceutical drugs.9 A QSAR is simply a mathematical equation that is derived from a set of molecules with a known activity using computational techniques. A variety of statistical approaches and computed molecular descriptors may be employed to

identify the exact form of the relationship between structure and activity, and this relationship is subsequently employed to predict the activity of new compounds. 10,11 QSAR investigations are based on the notion that changes in bioactivity are related with structural and molecular variation in a group of molecules. 12 The three-dimensional quantitative structure-activity relationship is one of the most successful and valuable strategies for the development and design of potent medications (3D-QSAR). 13

The goals of this research are to develop new neuraminidase inhibitors for the treatment of influenza. In a 3D-OSAR study based on a series of biologically active thiazolidine-4-carboxylic acid derivatives, we used comparative molecular field analysis (CoMFA) to find a statistically significant relationship between the three-dimensional structure of the molecules and their biological activity. After designing these molecules, we performed a docking study to arrange them in the active site of neuraminidase based on their stability. To identify the molecules with the best pharmacological properties, the compounds identified were also subjected to in silico absorption, distribution, metabolism, elimination, and toxicity (ADMET) property testing. We used ProToxII to assess the potential toxicity of all proposed molecules. Finally, we provided a reaction mechanism for the synthesis of each of these proposed compounds for future research into neuraminidase inhibitors.

2. Materials and Methods

2. 1. Experimental Databases

A set of twenty-five thiazolidine-4-carboxylic acid derivatives reported by Asadollah, M et al and Yu. L et al were chosen for molecular modelling studies. 14,15 Thiazolidine-4-carboxylic acid is a cyclic sulfur amino acid with a molecular structure similar to proline, hence the name thioproline. The thiazolidine-4-carboxylic acid sulfhydryl group is essential in metabolism as an antioxidant protector and in detoxification processes.¹⁶ Inhibitory activity was provided as IC50 values, which were then converted to pIC50 values [pIC50 = -log(IC50)] and used in 3D-QSAR experiments. All experimental data were divided into two categories: a training set for model generation and a test set for external evaluation of model accuracy, the training set contains twenty molecules and the test set contains five molecules. The variability of bioactivity rates and biological properties was also taken into account when randomly partitioning the training and test sets.¹⁷ (Table 1).

2. 2. Structure Preparation and Alignment

The SYBYL-X 2.0 software suite (Certara Enhances SYBYL-X Drug Design and Discovery Software Suite) was used to construct and optimise the structures of the twenty-five compounds with energy minimization.¹⁸ The tripos standard force field was used, and a condition of 0.01 kcal/

(mol) in Gasteiger-Hückel charge atomic partial was established. The tripos standard force field was used, and a condition of 0.01 kcal/(mol) in Gasteiger-Hückel charge atomic partial was established. ^{19,20} Molecular alignment is the most sensitive component, and it has a significant impact on 3D-QSAR models. ²¹ The structures that have been minimised and aligned are used to create the 3D-QSAR model.

2. 3. Generation of 3D-QSAR by CoMFA

Our goal was to develop a predictive 3D-QSAR model using comparative molecular field analysis (CoM-FA). The CoMFA method is a useful 3D-QSAR tool that has been used successfully in several medicinal chemistry studies. One of the significant advantages of this approach is its immediate application in the examination of any structure-dependent biological characteristics.²² The CoMFA theory states that differences in a target property between chemicals are frequently associated with changes in the noncovalent fields that surround those structures. These fields, which are the electrostatic (Coulombic) and steric (Lennard-Jones) fields, are computed at regular intervals within a predetermined area.²³ Steric and electrostatic descriptors were generated using a tripos force field and an ordered divergence grid of 2 Å with a cutoff energy value of 30 kcal/mol.²⁴ All other parameters have been reset to their default settings.

2. 4. PLS analysis and Validations

PLS regression is a well-established multivariate method that has been widely used in a variety of chemical fields.²⁵ A PLS model was built for the training set, and the model was validated using the remaining test set. To be trustworthy and predictive, 3D-QSAR models should be validated by producing correct predictions for external data sets that were not used in the model's development.¹⁰ PLS can assess complex structure-activity data more realistically and efficiently determine how molecular structure affects biological activity.²⁶ As a result, we estimate the mode's predictive power using external validation. A QSAR model is predictive, according to Golbraikh and Tropsha, if the following conditions are met.²⁷

$$\begin{split} R^2_{pred} > 0.6, \quad \left[r^2 - r^2_0 \right] / \ r^2 < 0.1, \quad \left[r^2 - r'^2_0 \right] / \ r^2 < 0, \\ and \\ 0.85 < k < 1.15 \text{ or } 0.85 < k' < 1.15 \end{split}$$

Roy and Paul developed the term $\rm r^2_m$ to verify the external predictability of the chosen model. ²⁷ An $\rm r^2_m$ value greater than 0.5 may be interpreted as indicating good external predictability.

The 3D-QSAR model was also validated using a Y-randomization test, which eliminates chance correlations between dependent and independent variables.²⁸ If the randomised models' correlation coefficient values R2

and Q2 are less than the original non-randomized model's R2 and Q2, we can be confident that the QSAR models are robust and not the result of random correlation.²⁹

2. 5. Molecular Docking

Molecular docking is a computational tool for determining the structure of a protein-ligand interaction automatically.³⁰ The true docking process, on the other hand, is so adaptable that receptors and ligands must adjust their conformation to match each other well.³¹ This technique has been widely used in the drug design research sector in recent years, and it also significantly increases efficiency and lowers research costs.³² One of the most famous molecular docking software packages, AutoDock Vina, combines a fast stochastic conformational search method with accurate and well-rated force-field-based and empirical scoring systems.^{33,34} The structure of neuraminidase was obtained from the RCSB database (PDB Id: 4ks2) Influenza neuraminidase in complex with an antiviral compound (1SJ)³⁵ as shown in the figure 1. In 1999, the Food and Drug Administration (FDA) approved Oseltamivir (italique) as a neuraminidase inhibitor.³⁶ As a second reference ligand, we docked Oseltamivir into the neuraminidase protein pocket. The receptors were then processed with UCSF Chimera 1.16 to remove non-standard residues before being docked using AutoDock Vina 1.1.2.37 The AUTOGRID system, which calculates ligand binding energy with their receptor, was used to define the three-dimensional grid.³⁸ The active site is located at coordinates (x = -23.4893 Å, y = 20.7720Å, and z = -9.6124 Å), and the grid size is x = 26.4819, y = 26.481925.6602, and z = 24.2547. The docking results were visualised using the Biovia discovery studio visualizer.³⁹

2. 6. Prediction of ADMET Properties

Following the molecular docking of the designed compounds for influenza neuraminidase inhibition, the

Table 1. A Tabular analysis of relationship between structures of compounds and experimental Activity.

Compound	R ₁	R ₂	pIC ₅₀
01	C ₆ H ₅ -	Н	4.672
02	$(2-OH)C_6H_5-$	H	4.695
03	(2-COOH)C ₆ H ₅ -	H	4.742
04	$(4-CN)C_6H_5-$	H	4.631
05	$(2-NO2)C_6H_5-$	H	4.648
06	$(2-OH, 3-CH3O)C_6H_5-$	H	4.91
07	C_4H_3O-	H	4.366
08	C_6H_5-	ClCH ₂ CO-	5.123
09	$(2-OH)C_6H_5-$	ClCH ₂ CO-	5.234
10	$(2-COOH)C_6H_5-$	ClCH ₂ CO-	4.971
11	$(4-CN)C_6H_5-$	ClCH ₂ CO-	5.063
12	$(2-NO2)C_6H_5-$	ClCH ₂ CO-	5.116
13	(2-OH, 3-CH3O)C ₆ H ₅ -	ClCH ₂ CO-	5.101
14	C_4H_3O-	ClCH ₂ CO-	4.889
15	C_6H_5-	PhCH ₂ CO-	5.917
16	$(2-OH)C_6H_5-$	PhCH ₂ CO-	6.187
17	$(2-COOH)C_6H_5-$	PhCH ₂ CO-	5.717
18	$(4-CN)C_6H_5-$	PhCH ₂ CO-	5.607
19	$(2-OH, 3-CH3O)C_6H_5-$	PhCH ₂ CO-	5.79
20	C_4H_3O-	PhCH ₂ CO-	5.539
21	C_6H_5-	NH ₂ CH ₂ CO-	6.276
22	$(2-OH)C_6H_5-$	NH ₂ CH ₂ CO-	6.678
23	$(2-COOH)C_6H_5-$	NH ₂ CH ₂ CO-	6.553
24	(2-OH, 3-CH3O)C ₆ H ₅ -	NH ₂ CH ₂ CO-	6.854
25	C ₄ H ₃ O-	NH ₂ CH ₂ CO-	6.009

absorption, distribution, metabolism, and elimination are estimated using the SwissADME web server.⁴⁰ Furthermore, the ProToxII-II and VEGA QSAR platforms were used to assess potential toxicity.^{41,42}

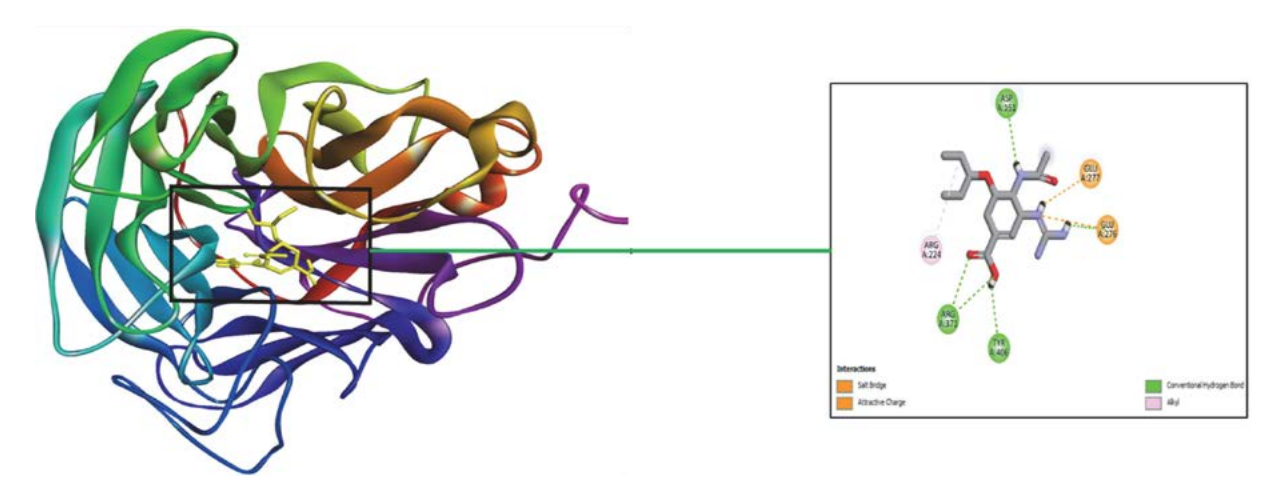


Fig. 1. Binding interaction illustration of Neuraminidase in complex with 1SJ.

3. Results and Discussions

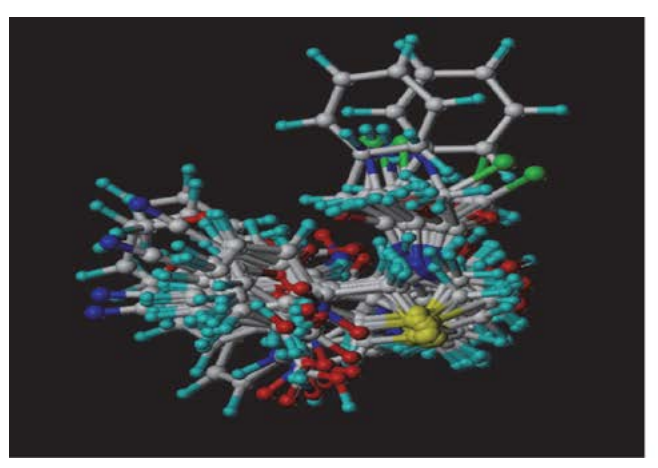
3. 1. Molecular Alignment of Dataset

Molecular alignment is one of the most important factors influencing the performance of 3D-QSAR approaches. ⁴³ The database was aligned for this phase using SYBYL-X 2.0 software, with the most active compound (compound 24, pIC50 = 6.780) serving as the structural template for the other compounds' alignment. Figure 2 shows the alignment of all molecules in the database (training and test set).

the CoMFA model developed is stable and has excellent predictive power.

Second, Table 3 shows the results of the CoMFA model's external validation. A high R2pred value greater than 0.6 indicates that the CoMFA model has good predictive power, and an R2m value of 0.778 indicates that the model has good predictive ability. Also, all values of ${\rm r^2}_0$ and ${\rm r'^2}_0$ are close to ${\rm r^2}$, $[{\rm r^2-r^2}_0]/{\rm r^2}$ and $[{\rm r^2-r'^2}_0]/{\rm r^2}$ have values much less than 0.1.

The Y-randomization test was performed fifty times to confirm the robustness of the CoMFA model. Table S1, shows



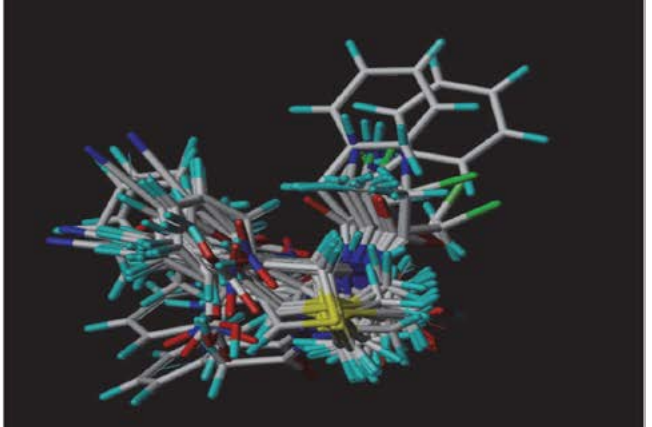


Fig. 2. The alignment of all molecules in the database (left: training set; right: test set).

3. 2. 3D-QSAR Model and Validations

The comparative molecular field method is used to establish a quantifiable link between the 3D structure of the compounds and their biological activity. Table 2 shows the statistical results of the PLS analysis for the CoMFA model. This CoMFA model has an extremely high R2 value of 0.997, the optimal number of components of 5, and an F-value of 883.433. Furthermore, the built model had a cross validated coefficient of Q2 of 0.708, with a very small standard error of estimation (SEE) of 0.050. The significant R2 and Q2 values, as well as the low SEE value, suggest that

the results of the Y-randomization test. The results show that the Q2 and R2 values obtained by the fifty random variations are lower than the values obtained by the original models. These findings show that the built model is reliable and did not result from random correlation of the training set.

TThe PLS results and the external validation show that the CoMFA model is reliable and statistically significant. The actual and predicted pIC50 values, as well as the residual values determined by the CoMFA model, are shown in Table S2. Figure 3 depicts the excellent correlation between actual and predicted activity, demonstrating the 3D-QSAR model's superior predictive ability.

Table 2. Statistical parameters of partial Least Squares (PLS) analysis on the comparative molecular field analysis (CoMFA) model.

Model	Q^2	\mathbb{R}^2	SEE	F	N	Fraction	
						Steric	Electrostatic
CoMFA	0.708	0.997	0.050	883.433	5	0.412	0.588

Table 3. Assessing the predictive performance by statistical parameters of external validation for the comparative molecular field analysis (CoMFA) model.

R ² _{pred}	r ²	$\mathbf{r^2}_0$	r'2 ₀	K	K'	$[r^2 - r^2_{0}]/r^2$	$[r^2 - r'^2_{0}]/r^2$	r² _m
0.674	0.957	0.922	0.955	1.016	0.982	0.036	0.001	0.778

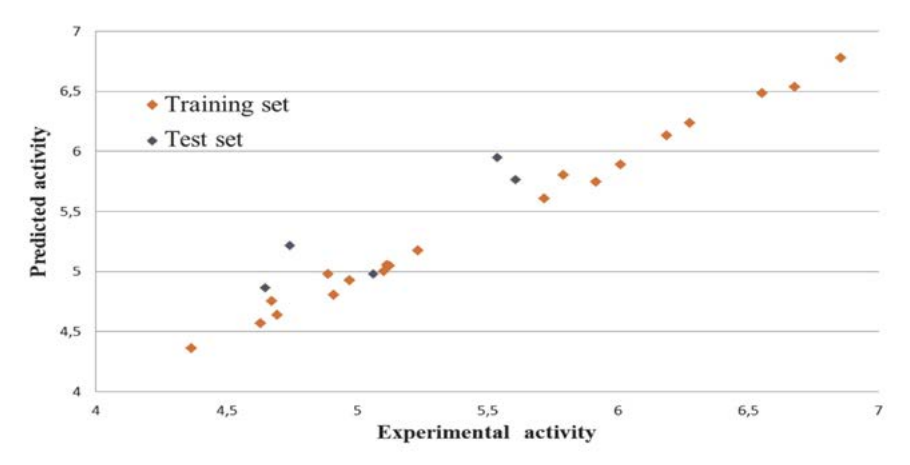


Fig. 3. The plot of the correlation between the experimental and predicted activity using 3D-QSAR model of training and test set.

3. 3. CoMFA Contour Map

The collected data were used to illustrate the favourable and unfavourable regions during which the structural changes of the compound result in an increase or decrease in biological activity for this critical phase. The steric and electrostatic contour maps generated by CoMFA modelling for the most active compound are shown in Figure 4. The green contours represent areas where bulky groups have a positive influence on neuraminidase inhibitory activity, whereas the yellow contours represent areas where bulky groups have a negative influence on inhibitory activity. Steric contour maps show the spatial volume of substituted groups in a variety of locations. Because of the presence of bulky groups in advantageous locations, it is possible that the steric effect influences the inhibitory activity of compounds 22, 23, and 24.

Blue and green regions are favorable for inhibitory activity, red and yellow green regions are unfavorable for inhibitory activity.

The blue contours indicate locations where electronegative groups positively influence neuraminidase inhibi-

tory activity, whereas the red contours indicate locations where electronegative groups negatively influence inhibitory activity. The contour map shows the presence of two large blue contour maps located between the nitrogen and sulfur atoms of the thiazolidine ring, as well as medium-sized contours near the aromatic ring. This helps to explain the higher activity of compound 24 with a methoxy group near the aromatic ring and the thiazolidine's NH2CH2CO- radical. This demonstrates that electronegative groups in these zones enhance the inhibitory activity of influenza virus. From these observations, it can be explained why the inhibitory activity of the best compounds to inhibit the vital function of neuraminidase.

3. 4. Design for New Neuraminidase Inhibitors

This study's primary goal is to develop new anti-influenza thiazolidine inhibitors. The CoMFA model contour map analysis provides useful information on structural properties for improving neuraminidase inhibitory

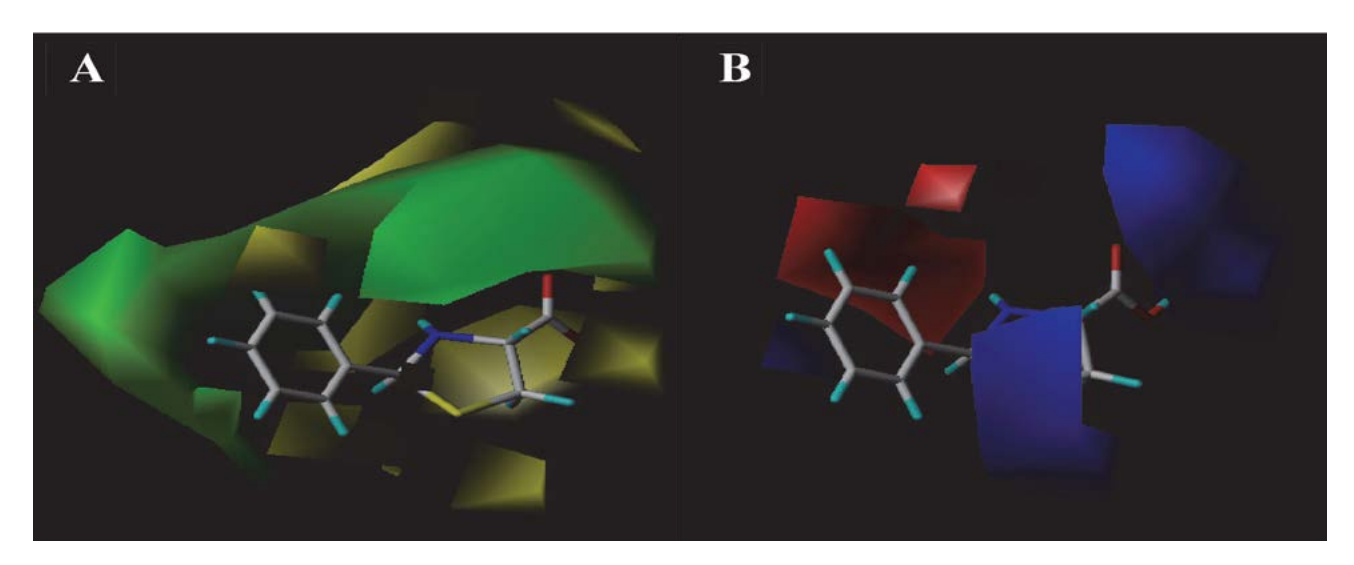


Fig. 4. CoMFA contour plot of compound binding to target: Visualization of (A) Steric and (B) Electrostatic Fields.

activity. Figure 5 depicts the collection of all orientations obtained from the CoMFA contour map, which proved to be a dependable and effective optimization strategy for the design of novel thiazolidines with high predicted inhibitory activity. Using a comparative molecular field, we created six (Th1-Th6) novel anti-influenza thiazolidine derivatives. Six molecules were optimised and aligned, with the most active compound acting as a structural template. Table 5 summarises the chemical structures and predicted pIC50 values of the novel compounds proposed. All six proposed compounds have higher predictive pIC50 values than the most active molecule (predictive pIC50 = 6,780for the most active compound). These molecules can be thoroughly investigated. Finally, as shown in figures 6 and 7, we proposed a reaction mechanism for synthesising these new molecules.

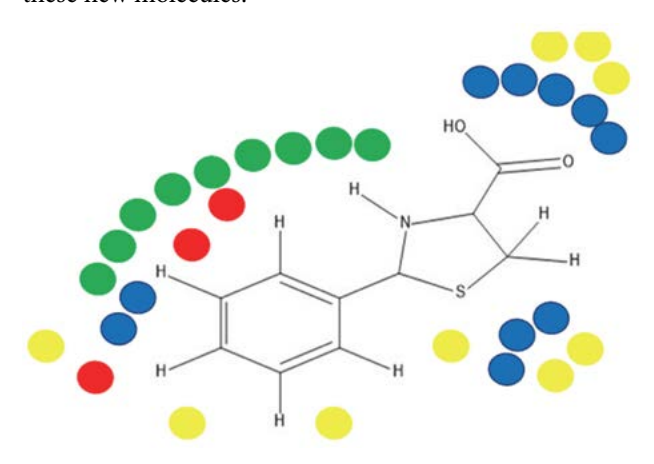


Fig. 5. Structural characteristics derived from CoMFA contour Map: Analysis of favorable and unfavorable regions for inhibitory activity. Blue and green regions are favorable for inhibitory activity, red and yellow green regions are unfavorable for inhibitory activity.

Fig. 6. Proposed reaction: General form and chemical equations.

3. 5. Molecular Docking

We performed molecular docking for the six designated molecules (Th1-Th6) to gain a better understanding of how the molecules obtained by 3D-QSAR inhibit the vital function of influenza virus neuraminidase, as well as the binding energy and types of interactions. Furthermore, we

Table 4. Structures and pIC_{50} values of novel molecules predicted by the CoMFA model.

Compound	Chemical structures	pIC ₅₀ predictive CoMFA	
Th1	OHOOH OH	7.036	
Th2	OH HONH2 NH2 NH2 NH2	7.638	
Th3	HO OH HO NH2 OH	7.090	
Th4	NH ₂ NH ₂ OH	7.211	
Th5	HO NH ₂ OH NH ₂	7.347	
Th6	HO HO NH ₂ OH	7.223	

docked Oseltamivir (italique) with neuraminidase to get a better estimate of the inhibitory efficacy of the proposed compounds (as another reference molecule). The docking modelling results for all proposed molecules and the neuraminidase inhibitor are presented in Table 7, and their types of interactions with the neuraminidase active site are shown in Figure 8. The results show that the designed compounds have binding affinity values ranging from –6.6 to –7.5 kcal/mol, while the binding affinity value of the reference compound (1SJ) is –6.6 kcal/mol, and the binding affinity value of Oseltamivir into neuraminidase is –6.6 kcal/mol. The interaction of the reference molecule (1SJ) and Oseltamivir with the active site of neuraminidase is depicted in Figure 9.

Fig. 7. Proposed general mechanism for synthesizing the six compounds: Insights into reaction pathways and synthetic strategies.

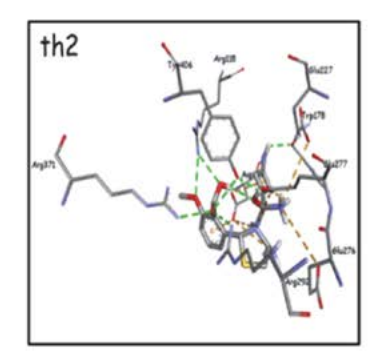
Th1, Th2, Th4, Th5, and Th6 have lower binding affinities than the reference molecule, indicating that this molecule is significantly more stable in the active site of neuraminidase. All of the molecules, including the reference compound, interacted with the amino acids Glu119, Asp151, Glu276 and Glu277 via Salt Bridge and Attractive Charge interactions.

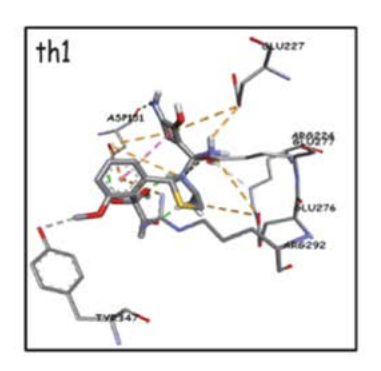
We observed a similarity of interaction for the two molecules with the highest binding affinity (Th2 and Th6), which interact with the amino acids Glu119, Trp178, Asp227, Glu277, and Tyr406. The reference molecule only interacts with the active site via a conventional hydrogen

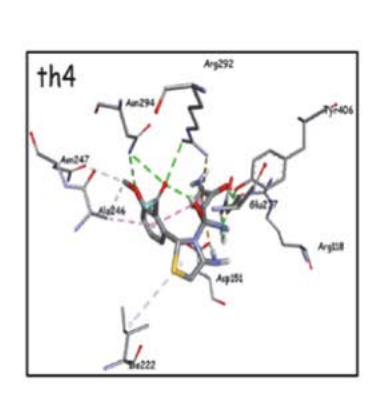
bond formed by the amino acids Asp151, Glu276 and Tyr406. It should be noted that conventional hydrogen bond interaction with the amino acids Glu119, Trp178, and Asp227 is critical for inhibiting the vital function of neuraminidase. The designed molecules Th1, Th2, Th4, Th5, and Th6 demonstrate significant binding to the active site of neuraminidase, confirming the 3D-QSAR model's good predictive power. Finally, our findings regarding the interactions between the six proposed molecules and the active site of neuraminidase agree with the findings of Gracy Fathima Selvaraj et al.⁴⁴

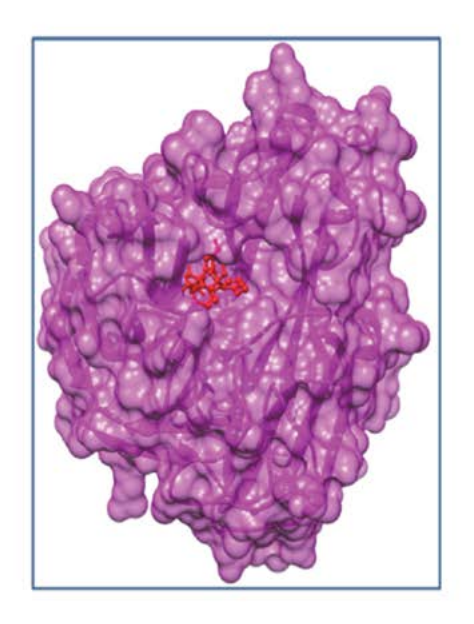
Table 5. Binding interactions and affinity values of six neuraminidase inhibitors within the active site.

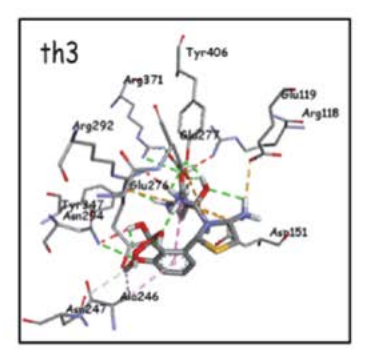
Ligand	Binding affinity (Kcal/mol)	Conventional Hydrogen Bond	Salt Bridge	Attractive Charge
Th1	-7.1	Asp151	Glu277	Asp151, Glu276, Glu277
Th2	-7.5	Asp277, Trp178, Glu277, Tyr406	Glu277	Asp151, Glu276, Glu277
Th3	-6.6	Glu276, Glu277, Tyr347, Tyr406	Asp151, Glu277	Glu119, Asp151, Glu277
Th4	-7.0	Asp151, Glu277, Tyr406	_	_
Th5	-6.9	Ala246, Tyr406	Asp151, Glu119, Glu277	Asp151, Glu119, Glu277
Th6	-7.5	Glu119, Trp178,Tyr406	Glu277	Asp151, Glu277
1SJ ref	-6.6	Asp151, Glu276, Tyr406	Glu277	Glu277
Oseltamiv	rir -6.6	Tyr406	_	Asp151, Glu119, Glu277

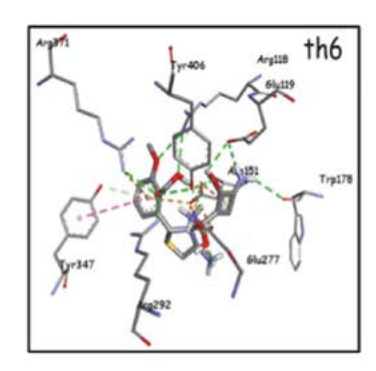












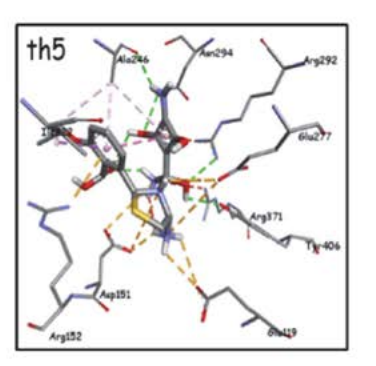
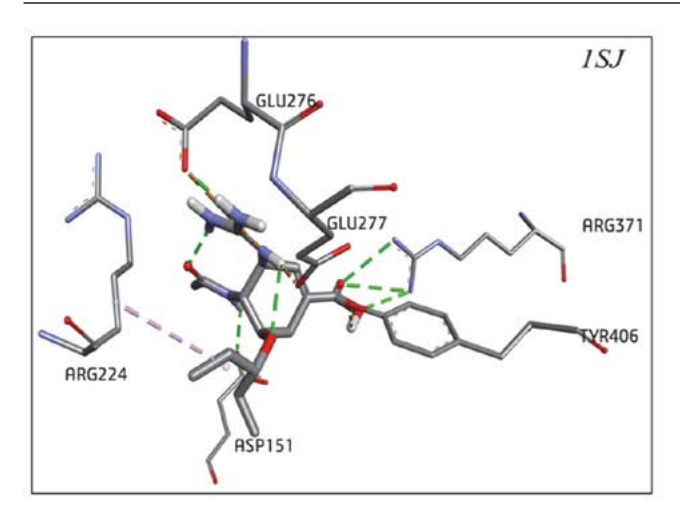


Fig. 8. Insights into ligand binding modes: Interactions of six designed compounds with neuraminidase active site.



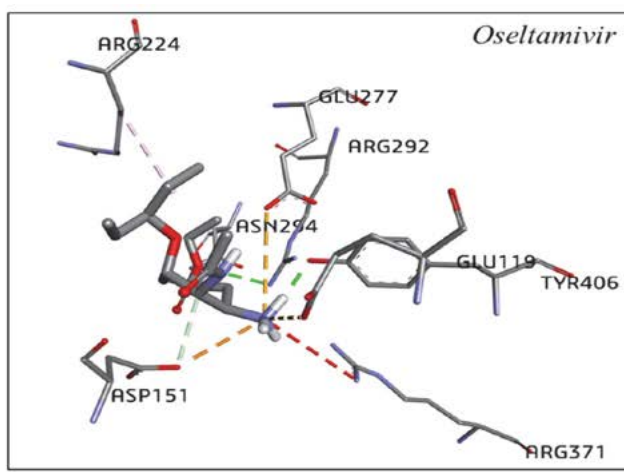


Fig. 9. Comparative analysis of ligand binding modes: Interactions of 1SJ (left) and Oseltamivir (right) with neuraminidase

3.6 ADMET and Bioavailability Prediction

This study was conducted to determine the critical pharmacokinetic parameters for the six designated molecules. The results obtained by SwissADME are shown in Table S3. All the molecules have LogP values between -1.30 and 0.06, these values indicate that all the molecules designed have good permeability towards biological membranes. For aqueous solubility, the six molecules have Log S values between -1 and 0, which means that all the molecules are easily soluble in aqueous media, according to these two parameters all the compounds have a good distribution. The six designed molecules (Th1-Th6) were estimated in silico using the five rules of Lipinski. It was that all molecules follows the Lipinski's rule. For the interactions with hepatic cytochrome P450, we did not record any interaction with them, which means that both molecules have a good metabolism. Another important parameter to quantify the pharmacokinetics of these designated molecules is the bioavailability score, the six molecules have the same bioavailability score (0.55), this value indicates that all the molecules will reach the blood circulation by the oral route (That is, both molecules are well absorbed.). For elimination, due to the aqueous solubility of six proposed compounds, they are readily eliminated renally. Also good LogKp (skin permeation) values between -10.94 and -8.55. Finally, all the proposed molecules are moderately easy to synthesize (the six molecules have synthetic accessibility values lower than 4.75).

For a quick assessment of drug-likeness, a bioavailability radar is provided. The Bioavailability radar takes into account six physicochemical properties. Lipophilicity, size, polarity, solubility, flexibility, and saturation are the parameters involved. For all molecules to be drug-like compounds, the bioavailability radar graph must be contained within a pink area. If the graph is in this pink area, the molecule has a drug-like compound. The bioavailability radar plots of the six compounds are shown in Figure 10. Th2 and Th4 are pharmaceutical candidates. Although there is a small deviation from area at the point of polar

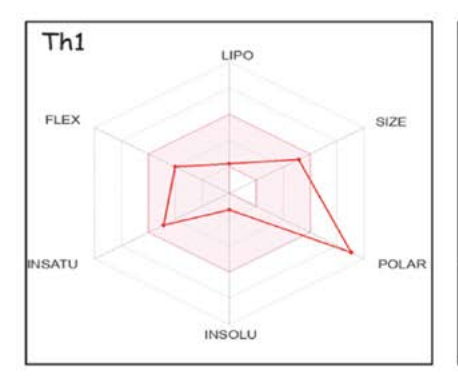
feature, Th1, Th3, Th5, and Th6 molecules are on the verge of being considered as drug candidates. These findings indicate that all molecules have very good bioavailability profiles.

We calculated the potential toxicity of these new molecules. Table S4, displays the ProToxII results. We found no evidence of toxicity caused by the designed compounds, whether it was Hepatotoxicity, Carcinogenicity, Immunotoxicity, Mutagenicity, or Cytotoxicity. With LD50 predictive values ranging from 230 to 8000 mg/kg and toxicity classes ranging from 2 to 4. We conclude that the molecules proposed using 3D QSAR are both safe and pharmacologically active.

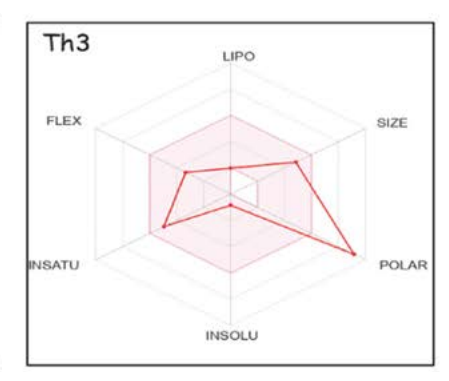
We estimated Mutagenicity (Ames test) model (CAESAR) 2.1.14, Developmental Toxicity (CAESAR) 2.1.8, Skin Irritation (CONCERT/Kode) 1.0.0, Plasma Protein Binding (- LogK, IRFMN) 1.0.0, P-Glycoprotein activity model (NIC) 1.0.1, and finally total body elimination half-life (QSARINS) 1.0.1 using VEGA QSAR. All of the obtained results are shown in Table S5. All predictions show that the six designed compounds are not mutagenic or toxic to development. Aside from that, none of these molecules cause skin irritation or infection. All molecules had plasma protein binding values ranging from -0.3285 to -0.0484. Furthermore, none of the six proposed compounds interact with P-Glycoprotein, which is found on the surface of biological cells. Furthermore, because their total body elimination half-life ranges between 1.533 and 2.837 hours, renal elimination of these molecules will be simple. The predicted toxicity study results show that all six proposed compounds are both safe and pharmacologically active.

4. Conclusion

A 3D-QSAR analysis of 25 thiazolidine-4-carboxylic acid derivatives was constructed in this study. This analysis was carried out by creating a 3D-QSAR model using the







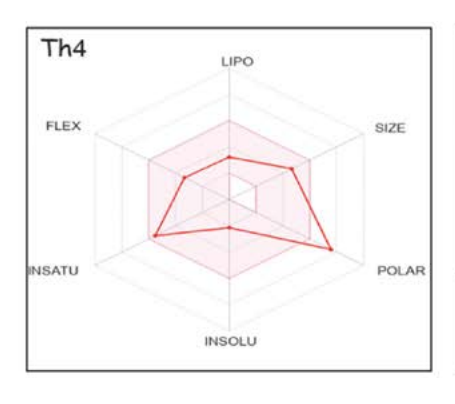






Fig. 10. Assessing Drug-like properties: Bioavailability radar graphs of six designed molecules.

CoMFA methodology. The derived 3D-QSAR models were validated using an external validation technique. We proposed six novel compounds with predicted inhibitory activity (pIC50) greater than the most active compound based on the information provided by the contour maps. All of the proposed compounds are more stable in the active site of neuraminidase than the reference molecule. however, Oseltamivir (italique) is more stable in the active site of neuraminidase (as second reference molecule). The molecular docking analysis confirms the 3D QSAR model's excellent prediction ability. Furthermore, we investigated the pharmacokinetic profile and potential toxicity of the six proposed compounds, and the results showed that each molecule follows Lipinski's rule and can be considered pharmacologically active and safe. We also presented a reaction mechanism for synthesizing these chemicals in order to conduct experimental research on their ability to suppress the critical function of neuraminidase and assess their efficacy in vitro and in vivo.

5. References

- 1. S. Lipničanová, B. Legerská, D. Chmelová, M. Ondrejovič, S, Miertuš, *Biomolecules* **2022**, *2*, 331–343.
 - DOI:10.3390/biom12020331
- J. Mauskopf, M. Klesse, S. Lee, G. Herrera-Taracena, Med. Econ. 2013, 2, 264–277.
 - DOI:10.3111/13696998.2012.752376

- R. Yoshida, M. Igarashi, H. Ozaki, N. Kishida, D. Tomabechi,
 H. Kida, K. Ito, A. Takada, *PLoS Pathog.* 2009, *3*, 1000350–1000359.
 DOI:10.1371/journal.ppat.1000350
- G. J. D. Smith, D. Vijaykrishna, J. Bahl, S. J. Lycett, M. Worobey, O. G. Pybus, S. K. Ma, C. L. Cheung, J. Raghwani, S. Bhatt, J. S. M. Peiris, Y. Guan, A. Rambaut, *Nature* 2009, 459, 2605–2615. DOI:10.1038/nature08182
- C. Seniya, G. J. Khan, R. Misra, V. Vyas, S. Kaushik, *Asian Pac. J. Trop. Dis.* 2014, 4, 1, 467–476.
 - **DOI:**10.1016/S2222-1808(14)60492-8
- A. Lackenby, T. G. Besselaar, R. S. Daniels, A. Fry, V. Gregory,
 L. V. Gubareva, W. Huang, A. C. Hurt, S. Leang, R. T.C. Lee,
 J. Lo, L. Lollis, S. Maurer-Stroh, T. Odagiri, D. Pereyaslov, E. Takashita, D. Wang, W. Zhang, A.Meijer, *Antivir. Res.* 2018, 157, 38–46. DOI:10.1016/j.antiviral.2018.07.001
- 7. M. G. Ison, *Clin. Chest. Med.* **2017**, *1*, 139–153. **DOI**:10.1016/j.ccm.2016.11.008
- 8. T. Jefferson, V. Demicheli, C. D. Pietrantonj, D. Rivetti, *Cochrane Database Syst. Rev.* **2006**.
 - DOI:10.1002/14651858.CD001169.pub3
- A. V. Veselovsky, A.S. Ivanov, Curr. Drug Targets Infect. Disord. 2003. 3, 33–40. DOI:10.2174/1568005033342145
- J. Verma, V. M. Khedkar, E. C. Coutinho, Curr. Top. Med. Chem. 2010, 10, 95–115. DOI:10.2174/156802610790232260
- S. Weaver, M. P. Gleeson, Mol. Graph. Model. 2008, 26, 1315–1326. DOI:10.1016/j.jmgm.2008.01.002
- A. Lavecchia, C. D. Giovanni, Curr. Med. Chem. 2013, 20, 2839–2860. DOI:10.2174/09298673113209990001
- 13. K. Nikolic, L. Mavridis, T. Djikic, J. Vucicevic, D. Agbaba, K.

- Yelekci, J. B. O. Mitchell, *Front. Neurosci.* **2016**, *10*, 265–296. **DOI**:10.3389/fnins.2016.00265
- 14. M. Asadollahi-Baboli, A. Mani-Varnosfaderani, *Med. Chem. Res.* **2013**, *22*, 1700–1710. **DOI:**10.1007/s00044-012-0175-y
- Y. Liu, F. Jing, Y. Xu, Y. Xie, F. Shi, H. Fang, M. Li, W. Xu, *Bioorg. Med. Chem.* 2011, *7*, 2342–2348.
 DOI:10.1016/j.bmc.2011.02.019
- H. U. Weber, J. F. Fleming, J. Miquel, Arch. Gerontol. Geriatr.
 1982, 4, 299–310. DOI:10.1016/0167-4943(82)90030-9
- A. D. Beirami, Z. Hajimahdi, A. Zarghi, *Biomol. Struct. Dyn.* 2018, 11, 2999–3006. DOI:10.1080/07391102.2018.1502687
- 18. TRIPOS Associates, Inc. **2012**, Sybyl-X molecular modeling software packages, version 2.1.1. https://www.certara.com/pressreleases/certaraenhances-sybyl-x-drug-designand-discovery-software-suite/
- H. Yuan, J. Zhuang, S. Hu, H. Li, J. Xu, Y. Hu, X. Xiong, Y. Chen, T. Lu, *Chem. Inf. Model*. 2014, 9, 2544–2554.
 DOI:10.1021/ci500268s
- M. Clark, R. D. Cramer, N. V. Opdenbosch, Comput. Chem. 1989, 8, 982–1012. DOI:10.1002/jcc.540100804
- H. Hong, H. Fang, Q. Xie, R. Perkins, D. M. Sheehan, W. Tong, SAR QSAR Environ Res. 2003, 18, 373–388
 DOI:10.1080/10629360310001623962
- A. Zieba, T. Laitinen, J. Z. Patel, A. Poso, A. A. Kaczor, *Int. J. Mol. Sci.* 2021, 22, 6108–6124. DOI:10.3390/ijms22116108
- 23. L. STAHLE, S. WOLD, *Prog. Med. Chem.* **1988**, 25, 291–338. **DOI:**10.1016/S0079-6468(08)70281-9
- 24. M. Baroni, G. Costantino, G. Cruciani, D. Riganelli, R. Valigi, S. Clementi, *Quant. Struct.-Act. Rel.* **1993**, *12*, 9–20. **DOI:**10.1002/qsar.19930120103
- L. El Mchichi, A. El Aissouq, R. Kasmi, A. Belhassan, R. El-Mernissi, A. Ouammou, T. Lakhlifi, M. Bouachrine, *Mater. Today: Proc.* 2021, 45, 7661–7674.
 DOI:10.1016/j.matpr.2021.03.152
- A. Golbraikh, A. Tropsha, Mol. Graph. Model. 2002, 20, 269–276. DOI:10.1016/S1093-3263(01)00123-1
- 27. R. Veerasamy, H. Rajak, A. Jain, S. Sivadasan, C. P. Varghese, R. K. Agrawal, *Int. J. Drug Discov.* **2011**, *3*, 511–519.
- K. Roy, Expert. Opin. Drug. Deliv. 2007, 2, 1567–1577.
 DOI:10.1517/17460441.2.12.1567
- C. Rucker, G. Rucker, M. Meringer, Chem. Inf. Model. 2007, 47, 2345–2357. DOI:10.1021/ci700157b
- 30. R. Dias, W. F. D. Azevedo Jr, *Curr. Drug. Targets*, **2008**, *9*, 1040–1047. **DOI:**10.2174/138945008786949432
- 31. J. Fan, A. Fu, L. Zhang, *Quant. Biol.* **2019**, *2*, 83–89. **DOI:**10.1007/s40484-019-0172-y
- F. D. Prieto-Martínez, E. L. Lopez, K. E. J. Mercado, J. L. Medina-Franco, *In Silico Drug Des.* 2019, 20, 19–44.
 DOI:10.1016/B978-0-12-816125-8.00002-X
- 33. O. Trott, A. J. Olson, *Comput. Chem.* **2009**, *31*, 455–466. **DOI:**10.1002/jcc.21334
- V. Temml, Z. Kutil, Comput. Struct. Biotechnol. J. 2021, 19, 1431–1444. DOI:10.1016/j.csbj.2021.02.018
- B. Acharya, S. Ghosh, H. K. Manikyam, *Pharm. Sci. Res*, 2016, 6, 2699–2719. DOI:10.13040/IJPSR.0975-8232.7(6).2699-19
- 36. Q. Tan, L. Duan, Y. Ma, F. Wu, Q. Huang, K. Mao, W. Xiao,

- H. Xia, S Zhang, E. Zhou, P. Ma, S. Song, Y. Li, Z. Zhao, Y. Sun, Z. Li, W. Geng, Z. Yin, Y. Jin, *Bioorg. Chem.* **2020**, *104*, 104257–104257. **DOI:**10.1016/j.bioorg.2020.104257
- D. Seeliger, B. L. G. Groot, J. Comput. Aided. Mol. Des. 2010, 24, 417–422. DOI:10.1007/s10822-010-9352-6
- G. M. Morris, D. S. Goodsell, R. S. Halliday, R. Huey, W. E. Hart, R. K. Belew, A. J. Olson, *Comput. Chem.* 1998, 14, 1639–1662.
 - **DOI**:10.1002/(SICI)1096-987X(19981115)19:14<1639::AID-JCC10>3.0.CO;2-B
- S. Sharma, P. Kumar, R. Chandra: Molecular Dynamics Simulation of Nanocomposites Using BIOVIA Materials Studio, Lammps and Gromacs, 2019, 39–100.
 DOI:10.1016/B978-0-12-816954-4.00007-3
- 40. A. Daina, O. Michielin, V. Zoete, *Nature* **2017**, *7*, 42717–42720. **DOI:**10.1038/srep42717
- P. Banerjee, A. O. Eckert, A. K. Schrey, R. Preissner, *Nucleic Acids Res.* 2018, 46, 257–263. DOI:10.1093/nar/gky318
- 42. Benfenati E, Manganaro A, Gini G. **2013**, *1107*, 21–28. http://www.vegahub.eu/portfolio-item/vega-qsar/. Accessed 12 April 2019
- 43. A. Zieba, T. Laitinen, J. Z. Patel, A. Poso, A. A. Kaczor, *Int. J. Mol. Sci.* **2021**, *22*, 6108–6114. **DOI:**10.3390/ijms22116108
- 44. G. F. Selvaraj, S. Piramanayagam, V. Devadasan, S. Hassan, K. Krishnasamy, S. Srinivasan, *Inform. Med. Unlocked* **2020**, *18*, 100284–10095. **DOI:**10.1016/j.imu.2019.100284

Povzetek

Cilj te raziskave je bil ustvariti model 3D-QSAR CoMFA za nabor petindvajsetih zaviralcev nevraminidaze, ki vsebujejo derivate tiazolidin-4-karboksilne kisline, in identificirati nov močan zaviralec nevraminidaze za zdravljenje gripe. Statistični parametri generiranega modela so odlični: Q2 = 0,708, R2 = 0,997. Rezultati zunanje validacije so bili (r_0^2 = 0.922, K = 1.016, R_{pred}^2 = 0.674, R_{m}^2 = 0.778), kar kaže, da ima izdelani model dobro napovedno vrednost. Na podlagi konturne karte modela CoMFA smo predlagali šest novih spojin z večjo inhibitorno aktivnostjo za nevraminidazo kot najbolj aktivna spojina. Te spojine smo s tehniko molekulskega sidranja ugnezdili v nevraminidazo, da bi analizirali interakcije z aktivnim mestom encima. Ugotovili smo, da so vse predlagane molekule bolj stabilno ugnezdene v aktivno mesto nevraminidaze kot referenčna molekula (1SJ). Uporabili pa smo tudi tehniko SwissADME za oceno farmakokinetičnih lastnosti vsake predlagane molekule, medtem ko smo za raziskovanje morebitne toksičnosti uporabili tehniki ProToxII in VEGA QSAR. Na koncu opisujemo reakcijski mehanizem za sintezo šestih predlaganih spojin, ki bi ga lahko še dodatno proučili pri iskanju novih inhibitorjev nevraminidaze. Ta študija je identificirala potencialne kandidate za razvoj učinkovitejših zaviralcev nevraminidaze za zdravljenje gripe.



Except when otherwise noted, articles in this journal are published under the terms and conditions of the Creative Commons Attribution 4.0 International License